Development of synthetic diagnostics for Fast Ion Loss Detection systems in Wendelstein 7-X

A. LeViness[1], S. A. Lazerson[2], A. Jansen van Vuuren[3], J. Rueda-Rueda[3], S. Bozhenkov[2], M. Garcìa-Muñoz[3], C. Killer[2], K. Ogawa[4], N. Pablant[1], and the W7-X Team

[1] *Princeton Plasma Physics Laboratory, Princeton, NJ, United States*

[2] *Max Planck Institute for Plasma Physics, Greifswald, Germany*

[3] *University of Seville, Seville, Spain*

[4] *National Institute for Fusion Science, Toki, Japan*

The Monte Carlo codes BEAMS3D [1] and ASCOT5 [2] are used to develop a synthetic diagnostic for a fast ion loss detector (FILD) in Wendelstein 7-X in order to simulate expected time-dependent signals from lost fast ions created by neutral beam injection (NBI). The method is validated against FILD data from the 2018 experimental campaign OP1.2b. This is the first quantitative agreement found between simulations and measured fast ions in W7-X.

The Wendelstein 7-X stellarator was optimized for good confinement of fast particles at high plasma pressure. Measurement of fast ion losses in W7-X is important in order to ascertain the success of the optimization, and comparison to simulations is necessary in order to validate the codes used to predict fast ion confinement both in W7-X and in future stellarators.

One method of measuring fast ion losses is through the use of FILDs, diagnostics that typically directly capture fast ions, measuring either the current produced in a thin plate (Faraday cup) or the light produced by fast ions impinging onto a phosphorescent material (scintillator). There are three FILDs either utilized on W7-X or planned for the near future:

- the NIFS-FILD, a Faraday cup FILD developed by the National Institute for Fusion Science (NIFS) with the Max Planck Institute for Plasma Physics (IPP), which was mounted on the multipurpose manipulator (MPM) for experiments during OP1.2b and OP2.1 [3]
- the FC-FILD, a Faraday cup FILD developed at IPP in collaboration with Princeton Plasma Physics Laboratory (PPPL) and implemented beginning in OP2.1 [4]
- the S-FILD, a scintillating FILD under development by PPPL, IPP, and the University of Seville, planned for the upcoming campaign OP2.2 [5]

The method presented here has been developed for the NIFS-FILD. It will be adapted in future work to simulate the FC-FILD and S-FILD, and to contribute to the design of the latter.

The difficulty in simulating FILD measurements is the impracticality of simulating a sufficiently large number of markers (simulated fast ions) in order for any to reach the miniscule

pinhole entrance of the FILD. Because of this, the method described in this paper aims to develop an efficient simulation method to allow high fidelity simulation of fast ions arriving at the detector while using a computationally tractable number of simulation markers. An artificial plane is constructed in front of the probe head, catching markers arriving from the last closed flux surface (LCFS). Meanwhile, separate simulations are used to determine the probability of any particle making it from the plane through the pinhole and onto one of the sensors.

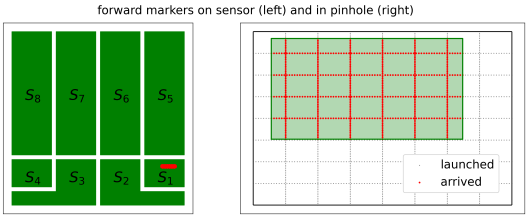

Figure 1: *Markers launched forward from the pinhole, those reaching S_1 shown in red.*

Markers are launched from the pinhole of the NIFS-FILD and followed backwards and forwards in time using ASCOT5. The markers at the pinhole are defined by normalized momentum $\rho_L = \frac{mv}{|q|B} = \frac{v}{v_\perp} r_{gyro}$, pitch angle $\chi = \cos^{-1}(\frac{v_\parallel}{v})$, and gyrophase ζ, each one calculated using the magnetic field given by ASCOT5 at the center of the pinhole.

In both simulations, markers are initialized in the pinhole in sets with discrete values of (χ,ρ_L,ζ). Those launched forwards are tracked until they stop, either being collimated by the aperture structure or landing on one of the eight sensors within the detector. They are initialized in a cross-hatch pattern, which makes it easy to find the outline of the region within which markers will arrive onto the sensor, as seen in Figure 1. The probability of a marker with (χ,ρ_L,ζ) beginning anywhere within the pinhole reaching the sensor tile S_1 is thus the green shaded area in Figure 1 divided by the total area of the pinhole:

$$P_{\chi,\rho_L,\zeta}(pin \rightarrow S_1) = \frac{A_{green}}{A_{pin}} \quad (1)$$

The markers launched backwards are followed until they are shadowed by the probe head or they collide with an artificial plane constructed at constant toroidal angle ϕ behind the pinhole. They are initialized in lines at the top and bottom edges of the pinhole, forming an outline of the pinhole which is projected onto the plane, as seen in Figure 2 (top).

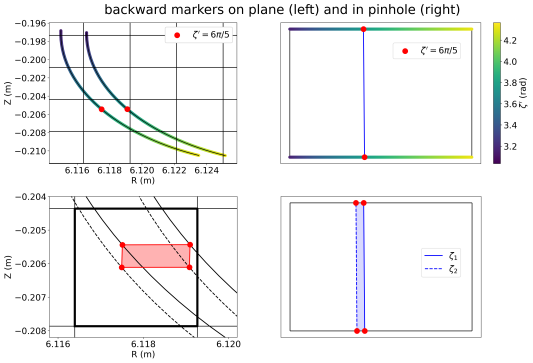

Figure 2: *Markers launched backwards from the pinhole towards the virtual plane.*

Markers at the plane are defined by $(R, Z,\chi,\rho_L,\zeta')$, where ζ' is the gyrophase at the virtual plane. It is assumed that χ and ρ_L do not change in the time of flight to the plane, which is less than a full gyro-orbit. To convert from ζ to ζ', we need to include a second set of initial markers. Our original set of markers has (χ,ρ_L,ζ_1), while the second set, represented by the dashed lines in Figure 2 (bottom), is initialized with (χ,ρ_L,ζ_2).

For each set, the two markers with our specified ζ' at the plane are chosen.

These four markers form polygons both at the plane and within the pinhole, as seen in Figure 2 (bottom). The probability of a marker with (χ,ρ_L,ζ') which is launched in the bold *R-Z* box arriving at the pinhole with $\zeta \in [\zeta_1, \zeta_2]$ is the red shaded area divided into the area of the *R-Z* box. It will "see" a reduced pinhole denoted by the blue shaded area.

$$P_{R,Z,\chi,\rho_L,\zeta'}(plane \rightarrow pin \cap \zeta \in [\zeta_1, \zeta_2]) = \frac{A_{red}}{A_{RZ\,box}} \tag{2}$$

These results can be combined with the forward simulations to find the full probability of transmission through the pinhole. Both marker sets are followed forward as well as backward, and the intersection between each blue line (representing markers with a given (ζ',ζ) pair) and each green rectangle (representing markers with each ζ which can reach sensor S_1) is determined. These intersection points are combined to form a new polygon, as seen in Figure 3.

The probability that markers which begin at the plane with ζ' and arrive at the pinhole with $\zeta \in [\zeta_1, \zeta_2]$ will make it to sensor S_1 is the purple shaded area divided into the blue shaded area:

$$P_{\chi,\rho_L,\zeta'}(pin \rightarrow S_1 \,|\, \zeta \in [\zeta_1, \zeta_2]) = \frac{A_{purple}}{A_{blue}} \tag{3}$$

Finally, these probabilities can be combined to find the desired answer: for a marker which begins at the plane within the specified *R-Z* box with (χ,ρ_L,ζ'), what is the probability it will pass through the pinhole and land on sensor S_1?

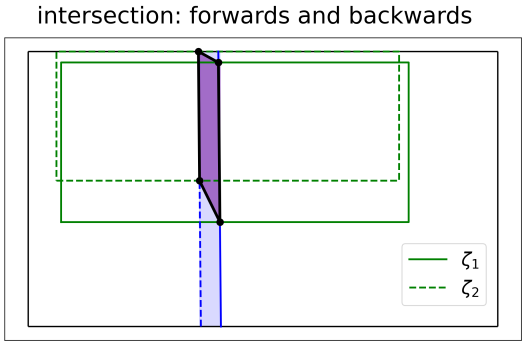

Figure 3: *The intersection of areas for viable forward and backwards markers within the pinhole.*

The probability it will pass through the pinhole with $\zeta \in [\zeta_1, \zeta_2]$ and land on sensor S_1 is

$$P_{R,Z,\chi,\rho_L,\zeta'}(plane \rightarrow S_1 \cap \zeta \in [\zeta_1, \zeta_2]) = \frac{A_{red}}{A_{RZ\,box}} \cdot \frac{A_{purple}}{A_{blue}} \tag{4}$$

and in order to get the total probability, one must sum over every value of ζ at the pinhole:

$$P_{R,Z,\chi,\rho_L,\zeta'}(plane \rightarrow S_1) = \sum_i P_{R,Z,\chi,\rho_L,\zeta'}(plane \rightarrow S_1 \cap \zeta \in [\zeta_i, \zeta_{i+1}]) \tag{5}$$

In order to bin the probability in (χ,ρ_L,ζ'), we average over several values of each quantity within a chosen bin. The result is a 6D probability matrix $P(S,R,Z,\chi,\rho_L,\zeta')$ which can be applied to any markers reaching the plane. A separate simulation is performed to get the arriving lost ions. BEAMS3D is used to simulate deposition and slowing down of the NBI fast ions, which are followed until they thermalize or escape through the LCFS. From each lost marker,

100 new markers are created, given a random gyrophase and a small perturbation in pitch, and followed to the wall using full-orbit ASCOT5. When a marker passes through the plane, it is saved but not stopped. These markers will form the simulated signal.

In order to increase statistics of simulated ions, it is necessary to further increase the number of markers. This is done by taking each saved marker, creating a circle around the gyro-center of radius $r = |\sin\chi|\rho_L$ (the traditional gyroradius), and creating a large number of new markers (500 for this example) with a proportionally reduced weight, evenly distributed around the circle, with the same χ and ρ_L, but new ζ'. Each resulting marker is then sorted into a bin in $(R, Z, \chi, \rho_L, \zeta')$, and the marker's weight is multiplied by $P(S, R, Z, \chi, \rho_L, \zeta')$, resulting in the marker's contribution to each of the channels of the detector. This is combined with the arrival time of each marker and the length of the NBI to produce a signal for each channel:

$$S_i(t) = \sum_j q_j w_j P(S_i, R_j, Z_j, \chi_j, \rho_{L_j}, \zeta'_j) \cdot [H(t - t_{0j}) - H(t - (t_{0j} + T_{NBI}))] \tag{6}$$

where j represents each marker, q_j its charge, w_j its weight, and H the Heaviside step function.

The simulated signal for Channel 1 of the NIFS-FILD during shot 20180918.045, from the 10 ms NBI blip beginning at 4.7 s, is shown in Figure 4 and compared to the experimental data, which has been averaged over four NBI blips between 4.7 and 5.1 s. The experimental signal was conditioned by filtering out 50 Hz noise and subtracting a background. The simulated signal has been shifted forwards 1.5 ms in time. The close agreement between experiment and simulation validates the use of this approach to simulate FILD diagnostics.

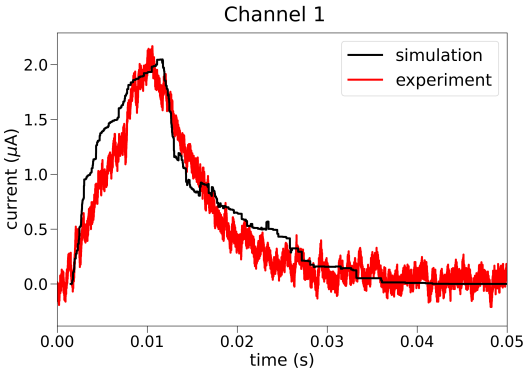

Figure 4: *Simulated and experimental NIFS-FILD signal for the W7-X shot 20180918.045.*

Acknowledgements

This work has been carried out within the framework of the EUROfusion Consortium, funded by the European Union via the Euratom Research and Training Programme (Grant Agreement No 101052200 — EUROfusion). Views and opinions expressed are however those of the author(s) only and do not necessarily reflect those of the European Union or the European Commission. Neither the European Union nor the European Commission can be held responsible for them. This work was funded by DoE contract number DE-AC02-09CH11466.

References

[1] M. McMillan and S. A. Lazerson, Plasma Phys. Control. Fusion **56**, 095019 (2014)
[2] J.A. Heikkinen and S.K. Sipila, Phys. Plasmas **2**, 3724 (1995)
[3] K. Ogawa *et al.*, J. Instrum. **14**, C09021 (2019)
[4] S. A. Lazerson *et al.*, Rev. Sci. Instrum. **90**, 093504 (2019)
[5] A. Jansen van Vuuren *et al.*, IEEE Trans. Plasma Sci. **50**, 4114 (2022)